BMC Medical Genomics

RESEARCH

Open Access

Elevated expression of APOO as a potential prognostic marker in breast cancer: insights from bioinformatic analysis and experimental validation

Yang Bai[1,3†], Qian Tang[4†], Liang Zheng[2†], Jun He[3], Wenjian Wang[1], Liqi Li[3*†] and Ju Yu[2*†]

Abstract

Objective Apolipoprotein O (APOO) has been identified through bioinformatic prediction analysis as being highly expressed in various tumors, including breast cancer (BRCA). However, further investigations are required to understand and confirm APOO's biological role in BRCA.

Methods Bioinformatic analyses were employed to identify genes' expression statuses and their relationship with the prognoses of patients. The genes' functions were determined in cell line by gain or loss of function assays. Mechanistic studies were carried out by western blot.

Results Our study reveals a correlation between increased APOO expression and poorer clinical outcomes in BRCA patients. The diagnostic value of APOO was demonstrated by Receiver Operating Characteristic (ROC) curve analysis, showing a notable area under the curve (AUC) of 0.937. Additionally, we observed that APOO knockdown impedes cell proliferation and migration. Gene Set Enrichment Analysis (GSEA) suggests that APOO expression is associated with the regulation of apoptosis and autophagy signaling pathways. Experimentally, modifying APOO expression in vitro influenced apoptosis and autophagy in BRCA cells. In conclusion, our findings indicate a significant link between APOO expression and BRCA progression, mediated through APOO's impact on cellular apoptosis and autophagy.

Conclusions Our data show that APOO controls BRCA process through apoptosis and autophagy signal pathway, which might provide multiple promising choices for the treatment of BRCA.

Keywords Apolipoprotein, Apoptosis, Autophagy, Breast cancer

†Yang Bai, Qian Tang, Liang Zheng, Liqi Li and Ju Yu contributed equally to this work.

*Correspondence:
Liqi Li
liliqi@tmmu.edu.cn
Ju Yu
yuju3@mail.sysu.edu.cn

[1]Laboratory of Department of Surgery, the First Affiliated Hospital of Sun Yat-sen University, Guangzhou 510080, Guangdong, China
[2]Department of Thyroid Surgery, the First Affiliated Hospital of Sun Yat-sen University, Guangzhou 510080, Guangdong, China
[3]Department of General Surgery, Xinqiao Hospital, Army Medical University, Chongqing 400037, China
[4]Department of Anesthesiology, Guiqian International General Hospital, Guiyang 550000, Guizhou, China

Introduction

Breast cancer (BRCA) remains a leading cause of cancer-related mortality among women, posing a substantial threat to women's health and well-being. In 2021, in the United States, BRCA constituted 30% of all cancer diagnoses in women [1]. Current research highlights the complexity of BRCA, indicating that the mechanisms behind different subtypes are not fully understood. Even within the same BRCA subtype, gene expression profiles can vary substantially, leading to differences in disease progression and prognosis among patients [2–5]. Therefore, it is crucial to screen for multiple BRCA subtypes and their expressed genes. This approach is vital for identifying tumor factors specific to each subtype, reducing treatment failures due to tumor heterogeneity, and improving the homogeneity in pathogenesis for each subtype. Such stratification can enhance the effectiveness of adjuvant therapies in BRCA and ultimately improve clinical outcomes for patients across various BRCA subtypes [6].

Lipid biosynthesis plays a critical role in regulating cell growth and proliferation, essential for growth, development, and maintaining cellular homeostasis [7]. Recent studies have identified an elevated risk of cancer in populations with metabolic disorders, typically marked by conditions like hyperlipidemia and hepatic steatosis. This correlation is underscored by findings that many cancers, including breast cancer (BRCA), demonstrate significantly increased lipid synthesis, deviating from normal cellular processes. This aberration in lipid production is an area of growing interest in cancer research, highlighting a potential link between metabolic dysregulation and oncogenesis [8].

APOO, a member of the apolipoprotein family, was first identified in 2003 in the hearts of dogs on a high-fat diet [9]. Officially named in 2006, APOO is implicated in lipid metabolism and inflammation [10]. It plays a crucial role in maintaining mitochondrial function, particularly as a part of the mitochondrial contact site and cristae organizing system (MICOS). This system is vital for stabilizing the folding of the mitochondrial inner membrane into cristae structures [11–13]. A notable function of APOO involves the uncoupling of mitochondria from ATP production, a process central to cellular energy management [11]. Furthermore, studies have shown that APOO can activate the MAPK signaling pathway in cardiac myocytes. This activation leads to autophagy and cell apoptosis, potentially exacerbating myocardial injury. These findings underscore the multifaceted role of APOO in cellular processes and its potential impact in various physiological and pathological contexts [14].

Despite advances in our knowledge, the primary functional role of APOO in BRCA remains elusive. Our research shows increased levels of APOO mRNA and protein expression in BRCA patients and cell lines. This observation leads us to hypothesize that elevated APOO expression could be a significant contributor to the initiation and progression of BRCA in vivo. To explore this hypothesis, our current study focuses on examining the effects of APOO on key cellular processes in BRCA, including cell migration, proliferation, apoptosis, and autophagy. This investigation aims to elucidate the role of APOO in BRCA pathophysiology and potentially guide future therapeutic strategies.

Materials and methods

Data Acquisition

Gene Expression Omnibus (GEO) dataset GSE3494, was used to acquire raw microarray mRNA expression data of BRCA patients. Additionally, we downloaded two datasets from The Cancer Genome Atlas (TCGA), including RNA-seq transcriptomic data and clinical information. Different groups of patients were classified based on APOO median expression levels. The thresholds of |log2 fold change (logFC)|> 1 and adjusted P value < 0.05.

GO/KEGG and GSEA enrichment analysis

Patients were divided into high-expression and low-expression groups based on the expression levels of APOO. Gene Ontology (GO), Kyoto Encyclopedia of Genes and Genomes (KEGG), and gene set enrichment analysis (GSEA) were performed based on the differentially expressed genes between the two groups. The aim of this analysis was to elucidate the potential biological functions and molecular mechanisms that distinguish the two APOO expression groups [15, 16].

Clinical statistical analysis

An analysis of progression-free intervals (PFIs), overall survival rates (OS), and disease-specific survival rates (DSSs) was conducted among patients in the TCGA, supported by 95% confidence intervals. To further explore the impact of APOO expression and other clinical characteristics on OS, we employed a Cox proportional hazards regression model. Based on the outcomes of the multivariate Cox analysis, we identified independent prognostic factors. These factors were then utilized to create nomograms. To assess the predictive accuracy and discriminative ability of these nomograms, we calculated the concordance index (C-index) and analyzed calibration curves. We also evaluated the predictive performance of these models by using the area under the Receiver Operating Characteristic curve (AUC).

Cell line cultivation

Human BRCA cell lines (SKBR-3, MCF-7, T- 47D, BT-474, ZR-7530, MDA-MB-157, MDA-MB-468) and the normal breast epithelial cell line (MCF-10 A) were

procured from the Cell Bank of the Chinese Academy of Sciences (Shanghai, China). The cell lines SKBR-3, T- 47D were cultured in DMEM (Gibco, USA). BT-474, ZR-7530 were cultured in RPMI-1640 (Gibco, USA). MDA-MB-157, MDA-MB-468 cell lines were cultured in L-15 Medium (Gibco, USA). The MCF-10 A cell line was cultured in MCF-10 A special medium (Procell, China). And at 37 °C under a 5% CO2 atmosphere, the cells were supplemented with 10% fetal bovine serum (Gibco, USA), along with 1% streptomycin and penicillin (Gibco, USA).

Cell transfection

SKBR-3 and ZR-7530 cells were plated in six-well plates and allowed to reach 60–70% confluence before transfection. siRNA for APOO and mRFP-GFP-LC3 adenoviral vectors were obtained from RiboBio (Guangzhou, China). And transfected into cells according to the manufacturer's protocol. Nonspecific siRNA or Vector was used as negative controls. The sequences of siRNA-APOO were as follows: siRNA-APOO-1 sense: 5′-GGUUAGACAGC UAUGACUA-3′, antisense: 5′-UAGUCAUAGCUGUCU AACC-3′; siRNA-APOO-2, sense: 5′-CUGAG GGUCAA UCGAAGUA-3′, antisense: 5′-UACUUCGAUUGACCC UCAG-3′; siRNA-APOO-3, sense: 5′-GGGUUUACGAG GAUAUAUA-3′, antisense: 5′-UAUAUAUCCUCGUAA ACCC-3′. Each siRNA was transfected into SKBR-3 and ZR-7530 cells and knockdown efficiency was assessed by RT-PCR. siRNA-APOO-1 and siRNA-APOO-2 were the most efficient as shown in Fig. 1B, and were chosen for further study.

qRT-PCR

Following the manufacturer's protocol, RNA was extracted using TRIzol (Invitrogen), then reverse-transcribed into complementary cDNA from the extracted RNA (1 μg) of each sample. The relative APOO level was calculated on basis of the expression of GAPDH level. The primers: APOO, forward 5′-CCTTCAAAGTCTAT GCAGCACC-3′ and reverse 5′-CCTTCAAAGTCTATG CAGCACC-3; GAPDH, forward 5′-GGAGCGAGATCC CTCCAA AAT −3′ and reverse 5′-GGCTGTTGTCATA CTTCTCATGG-3′.

Cell colony formation and proliferation assays

The proliferation ability of cell was measured using colony formation assay and Cell Counting Kit-8 (CCK8, TransGen, China) assays according to the kit's instructions. For the colony formation assays, siRNA-treated cell lines were seeded in 6-well plates and maintained in medium containing 10% FBS. We fixed the cells with 4% formaldehyde at the indicated timepoint (usually 2 weeks) and stained them with 0.1% crystal violet at room temperature for 30 min. We counted and compared the colonies only if colonies included at least 50 cells. For the CCK8 assay, the siRNA-treated cell lines (3×10^3 cells/well) were seeded in 96-well plates and CCK8 assay was performed every 24 h according to the manufacturer's instructions.

Wound closure assays

For wound closure assays, BRCA cells were seeded into 12-well plates (1.2×10^3 cells/well). At 48 h after siRNA transfection, scratch wounds were created using a sterilized 100 μL disposable pipette tip on single cell layer. Scratch wounds were visualized immediately and 24 h after wound cutting with an inverted microscope (ZEISS).

Western blot

Protein samples were extracted from total cells using RIPA lysis buffer (MIKX, China), and their protein concentration was determined using the BCA protein assay (Beyotime, China). Each sample was loaded with a total protein amount of 15–30 μg onto an 8–12% polyacrylamide gel. Following separation by SDS-PAGE, the samples were transferred onto a PVDF membrane and blocked with TBS buffer containing 0.05% Tween-20 (TBST) and 5% skimmed milk powder for a duration of 2 h. Subsequently, the membrane was incubated overnight at 4℃ with specific primary antibodies. The membrane was then incubated with corresponding secondary antibodies at room temperature for 1 h. Protein levels were visualized using chemiluminescence technology.

Cell migration analyses

BRCA cells migration were studied with Boyden chamber assays. Cell culture inserts with a PET membrane (2331805, Corning, USA) were used to perform Boyden chamber assays. After 48 h of siRNA transfection, the cells (1×105 cells) were suspended in medium without serum and then placed onto the upper chambers of the transwell insert. In the next step, the insert was inserted into a 24-well plate containing DMEM supplemented with 10% fetal bovine serum (Gibco, USA). After 24 h of incubation at 37℃, we fixed the membrane with paraformaldehyde (4%), and cotton swabs were used to remove the cells from the upper compartment, and 0.1% crystal violet was applied to the membrane surface. After three washes in PBS, we counted the migrated cells under an inverted microscope (Leica DMI4000B).

Cell cycle profile

Cell cycle analysis was performed using a cell cycle analysis kit. Breast cancer cells were collected and fixed with 70% ethanol at 4℃ for 2 h. In the following step, the cells were stained using a solution containing propidium iodide (0.05 mg/ml), RNase A (1 mg/ml), and 0.3% Triton X-100 for 30 min in the dark. In order to determine the

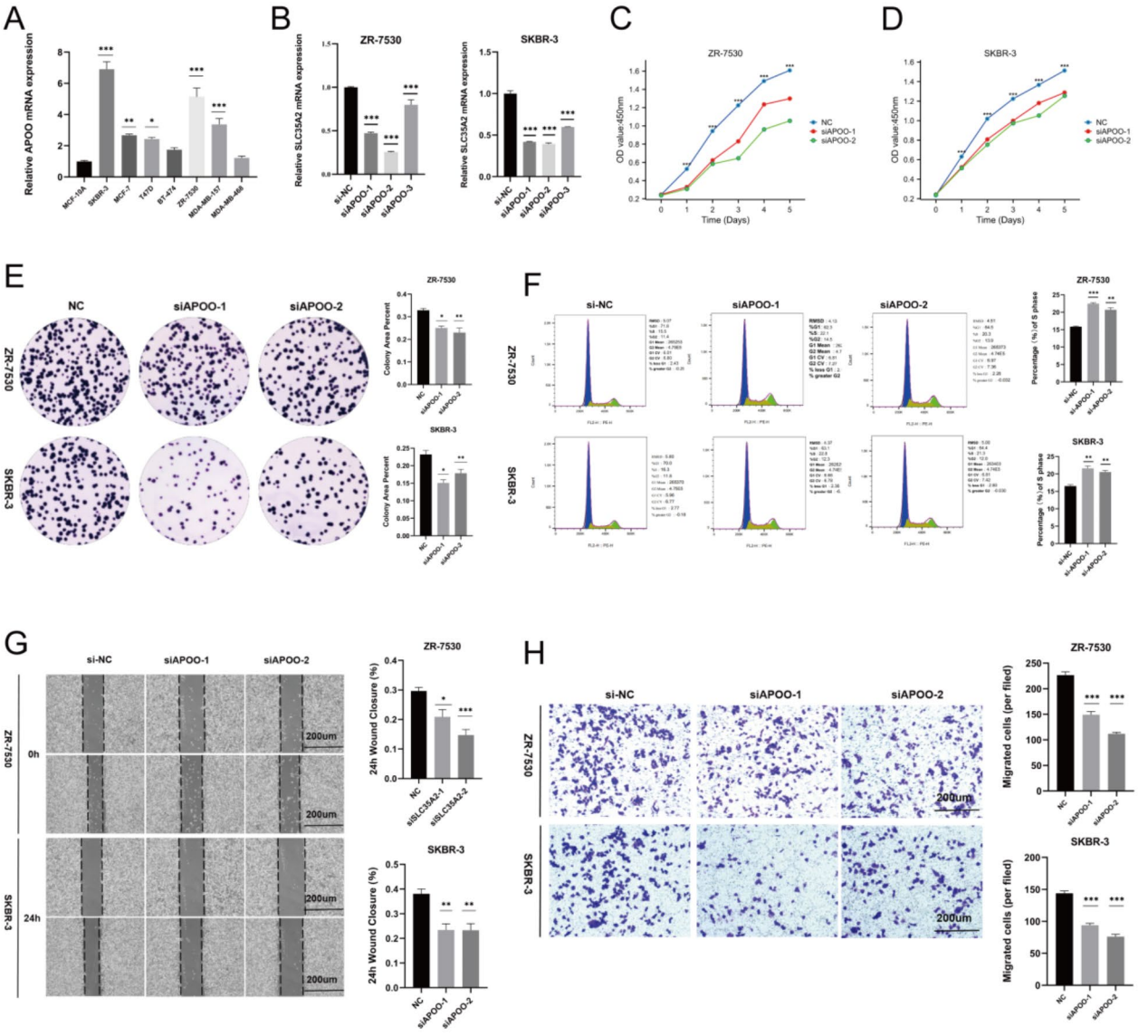

Fig. 1 APOO affects proliferation and migration of BRCA cell lines. (**A**)qRT-PCR was employed to identify the mRNA levels of APOO in SKBR-3, MCF-7, T- 47D, BT-474, ZR-7530, MDA-MB-157 and MDA-MB-468 cells. (**B**) qRT-PCR was used to detect the mRNA levels of APOO in SKBR-3 and ZR-7530 cells after silencing of APOO. (**C**-**D**) CCK8 assays were performed to test the survival SKBR-3 and ZR-7530 cells after silencing of APOO. (**E**) Colony formation experiments were conducted to test the survival SKBR-3 and ZR-7530 cells after silencing of APOO. (**F**) Flow cytometry was performed to test the cell cycle of SKBR-3 and ZR-7530 cells after silencing of APOO. (**G**) The number of migrated cells in different groups as determined via Transwell assays. (**H**) Wound healing assays assessing the migration of siAPOO-treated cells. (Scale bar = 200 μm) (*$p < 0.05$, **$p < 0.01$, ***$p < 0.001$)

percentage of cells in different phases of the cell cycle, the DNA content of cells was measured using flow cytometry (propidium iodide intensity). It was repeated three times independently for each experiment .

Apoptosis assays

For apoptosis assays, cells were harvested and stained with a TUNEL kit (Beyotime, China) according to the manufacturer's instructions.

Statistical analysis

All statistical analyses performed using GraphPad Prism (version 9.1.0) and R software (version 4.3.0) for Windows. Kaplan-Meier (KM) analysis was performed to determine survival outcomes. The median values were used as cut-off thresholds to plot the KM curves, and the statistical significance was evaluated by the log rank test. The Cox proportional hazard regression model was employed to perform univariate and multivariate analysis for OS. A nomogram for predicting the OS was built using the R library "rms" package. The survival

probabilities were predicted for both 1- and 3- and 5-year survival. Two-group comparisons were made using Student's t-tests, and multiple comparisons were made using one-way analysis of variance (ANOVA) or Kruskal-Wallis tests. Finally, to correct for multiple testing, we performed FDR correction on the p-values. All data are expressed as mean ± standard deviation. A *P*-value < 0.05 was deemed statistically significant.

Results

APOO expression in Pan-cancer and highly expressed in BRCA

Utilizing data from the TIMER database, we observed that APOO expression levels are notably elevated in various cancers, including BRCA (Fig. 2A-B). In paired sample analyses, a significant difference was observed between BRCA and adjacent normal tissues when APOO expression was compared ($p < 0.001$) (Fig. 2C). Furthermore, an analysis of TCGA BRCA patients was conducted to determine if APOO expression levels correlate with their clinical pathological characteristics. The analysis revealed increased APOO expression across all BRCA subgroups (**Figure S1A-I**).

Immunohistochemical staining data based on the Human Protein Atlas (HPA) further corroborated these findings, showing that APOO protein levels were upregulated in BRCA tissues (Fig. 2D). These observations collectively suggest that both mRNA and protein expression of APOO are elevated in BRCA.

To evaluate the diagnostic utility of APOO levels for BRCA, we employed ROC curve analysis. The AUC was 0.937, indicating that APOO possesses high sensitivity and specificity for BRCA diagnosis, as demonstrated in

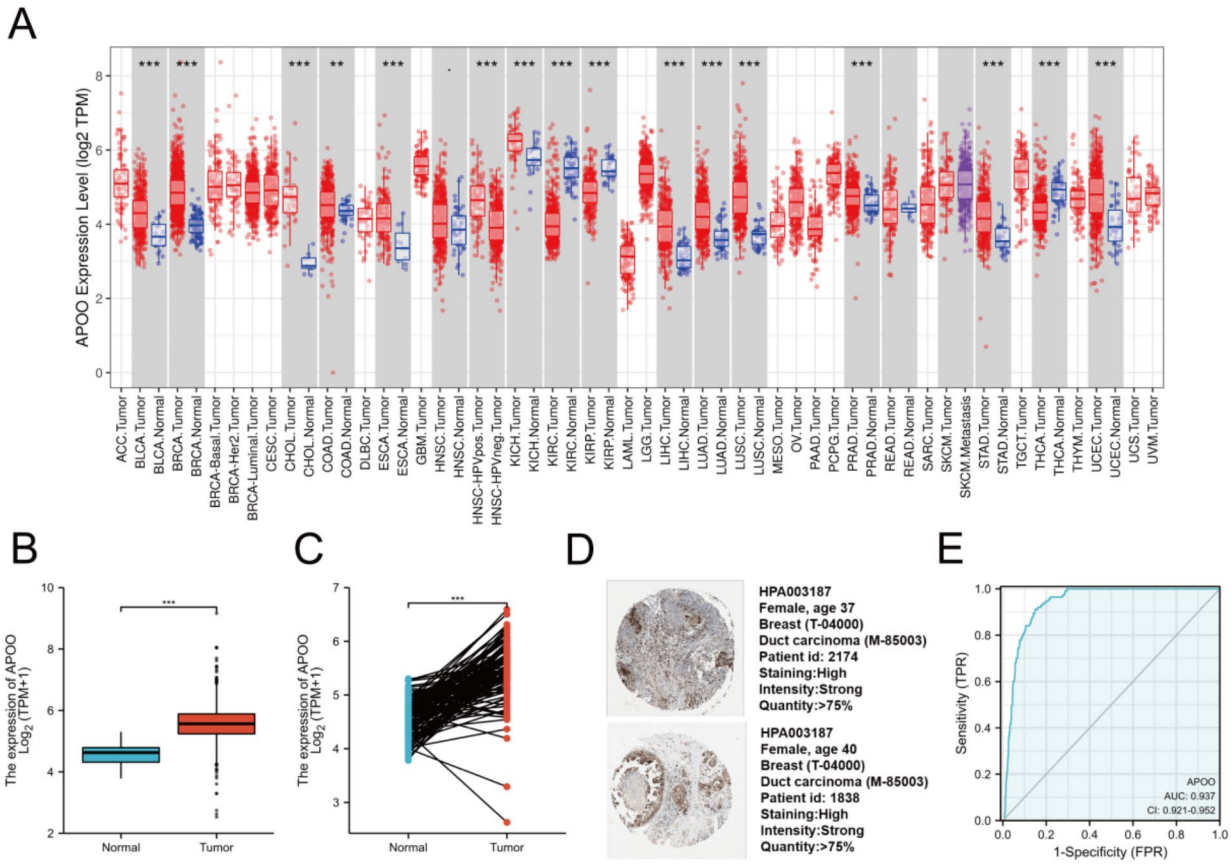

Fig. 2 High expression of APOO in malignant breast tissues is associated with poor prognosis in patients with BRCA. (**A**) Increased or decreased APOO in different tumor types from TCGA database were determined by TIMER. (**B**) APOO expression levels in BRCA and normal tissues. (**C**) APOO expression levels in BRCA and matched normal tissues. (**D**) APOO expression in BRCA tissues from HPA. (**E**) The ROC curve analysis of APOO in BRCA patients from TCGA database. (*$p < 0.05$, **$p < 0.01$, ***$p < 0.001$)

Fig. 2E. This highlights the potential of APOO as a biomarker for BRCA.

High APOO expression is associated with adverse outcomes in BRCA

In TCGA analysis, patients in the high APOO expression group exhibited significantly worse outcomes compared to those in the low APOO group across several metrics: OS (Hazard Ratio [HR]: 1.61, p=0.004), DSS (HR: 1.68,

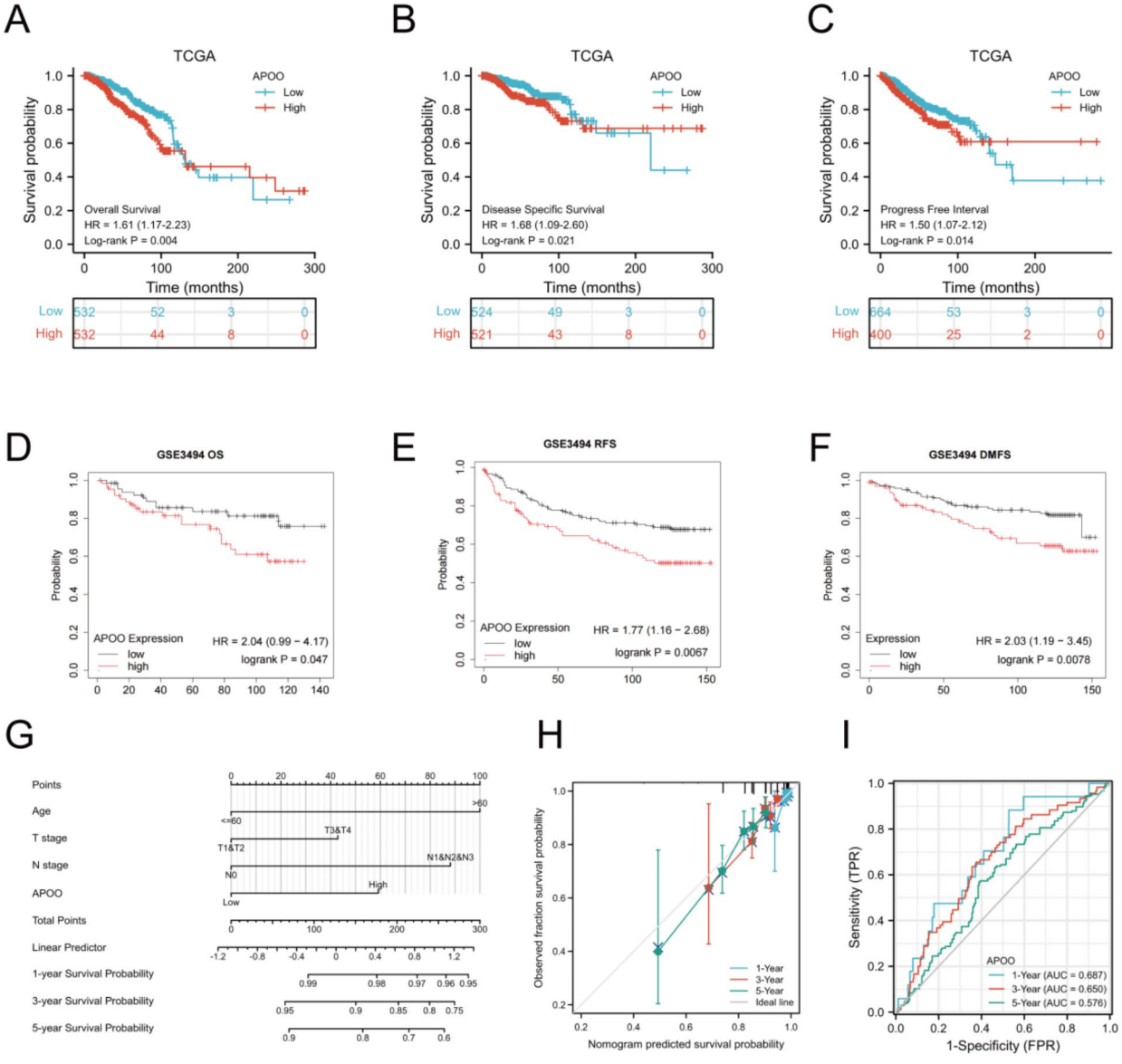

Fig. 3 High expression of APOO in malignant breast tissues is associated with poor prognosis in patients with BRCA. (**A**-**C**) TCGA survival curves for OS, DSS, and PFI. (**D**-**F**) Survival curves of OS, RFS and DMFS from GSE3494. (**G**) BRCA patient OS prediction nomogram based on 1-, 3-, and 5-year OS data. (**H**) Calibration plots of the nomogram. (**I**) ROC curves for this risk model in 1, 3, and 5 years

$p=0.021$), and PFI (HR: 1.50, $p=0.014$) (Fig. 3A–C). To confirm the link between APOO expression and OS, we conducted a similar analysis using the GSE3494 dataset. These results also indicated poorer OS in individuals with high APOO expression (Fig. 3D–F).

Further evaluation of APOO's prognostic value in clinical outcomes was conducted through univariable Cox regression analyses. To identify independent prognostic factors, all significant variables on univariate Cox regression analysis ($P \leq 0.05$) were subjected to multivariate Cox regression analysis. As presented in Table 1, APOO emerged as an independent risk factor for OS in both univariate (HR: 1.604, $p=0.004$) and multivariate Cox regression analyses (HR: 2.197, $p=0.002$). Utilizing significant prognostic factors from the multivariate analysis, including clinical T stages, N stages, and age, along with APOO, we constructed a prognostic nomogram to predict OS (Fig. 3G). The calibration curve assessed the nomogram's efficiency, revealing a C-index of 0.657. This indicates a high predictive accuracy (Fig. 3H) as well as the model's robust predictive performance (Fig. 3I).

To ascertain APOO's predictive value in clinical subgroups, Our study examined its association with OS across subgroups defined by different clinical characteristics. The analysis revealed that APOO expression was consistently associated with worse prognoses in subgroups including patients age>60 years, M0, N0, T1, ER+, PR+, Her2+, LumA, LumB, stage I–II, and non-radiotherapy groups, all statistically significant ($p<0.05$) as shown in Figure S2. This underscores APOO's potential as a significant prognostic biomarker in BRCA across diverse clinical scenarios.

Table 1 The prognostic covariates in patients with BRCA were analyzed using univariate regression and multivariate survival methods on overall survival

Characteristics	Univariate analysis		Multivariate analysis	
	Hazard ratio (95% CI)	*P* value	Hazard ratio (95% CI)	*P* value
T stage (T3&T4 VS. T1&T2)	1.608 (1.110–2.329)	**0.012**	2.989 (1.703–5.247)	**<0.001**
N stage (N1&N2&N3 VS. N0)	2.239 (1.567–3.199)	**<0.001**	1.846 (1.095–3.111)	**0.021**
M stage (M1 VS.M0)	4.254 (2.468–7.334)	**<0.001**	4.180 (1.704–10.255)	**0.002**
Age (> 60 VS.<=60)	2.020 (1.465–2.784)	**<0.001**	3.238 (1.972–5.318)	**<0.001**
PAM50 (Basal VS. LumA&LumB&Her2)	1.040 (0.695–1.558)	0.848		
PR status (Positive VS. Negative)	0.732 (0.523–1.024)	0.068		
ER status (Positive VS. Negative)	0.712 (0.495–1.023)	0.066		
HER2 status (Positive VS. Negative)	1.593 (0.973–2.609)	0.064		
APOO (High VS. Low)	1.604 (1.159–2.221)	**0.004**	2.197 (1.342–3.599)	**0.002**

Down-regulation of APOO affects the proliferation

Our analysis indicates that APOO is overexpressed in BRCA, with higher expression levels associated with a poorer prognosis. To further investigate APOO's biological functions in BRCA, we conducted cell experiments. Initially, we confirmed the high expression of APOO in BRCA cell lines using quantitative RT-PCR (qRT-PCR), particularly noting elevated levels in ZR-7530, SKBR-3, MCF-7, T-47D, BT-474, and MDA-MB-157 cells (Fig. 1A). Based on these findings, ZR-7530 and SKBR-3 cells, which exhibited the highest APOO expression, were selected for more detailed study.

ZR-7530 and SKBR-3 cells were transfected with siRNA targeting APOO to determine whether it affects BRCA cell migration. The efficiency of this transfection was confirmed through RT-qPCR analysis (Fig. 1B). Then, we performed CCK8 (Fig. 1C-D) and colony formation assays(Figs. 1E), which revealed that the down-regulation of APOO effectively inhibited proliferation in these BRCA cell lines. This led to the hypothesis that cells with reduced APOO expression would exhibit suppressed tumorigenic capabilities.

We further analyzed the effects of APOO on cell cycle distribution using flow cytometry. The results demonstrated that silencing APOO expression resulted in the number of cells in the G1 phase is significantly reduced while the number of cells in the S phase increases (Fig. 1F). This indicates that APOO significantly influences the cell cycle in both ZR-7530 and SKBR-3 cells, underlining its potential role in BRCA cell proliferation and tumorigenesis.

APOO promotes the Migration of BRCA cells

To determine the biological role of APOO in BRCA metastasis, we performed wound healing (Fig. 1G) and transwell experiments(Fig. 1H). The results showed that BRCA cells metastasized significantly less when APOO expression was inhibited. These results suggested that APOO is a metastasis-promoting gene in BRCA cells.

Functional Enrichment and analyses of APOO related genes in BRCA

KEGG/GO enrichment analysis was conducted to determine the functional enrichment of genes interacting with APOO (Fig. 4A). These analyses revealed that APOO-related genes are implicated in a diverse range of Cellular components (CCs), biological processes (BPs), and molecular functions (MFs), as well as various KEGG pathways. Notably, these genes are involved in the regulation of amine transport, highlighting their role in cellular transport mechanisms. Additionally, they are associated

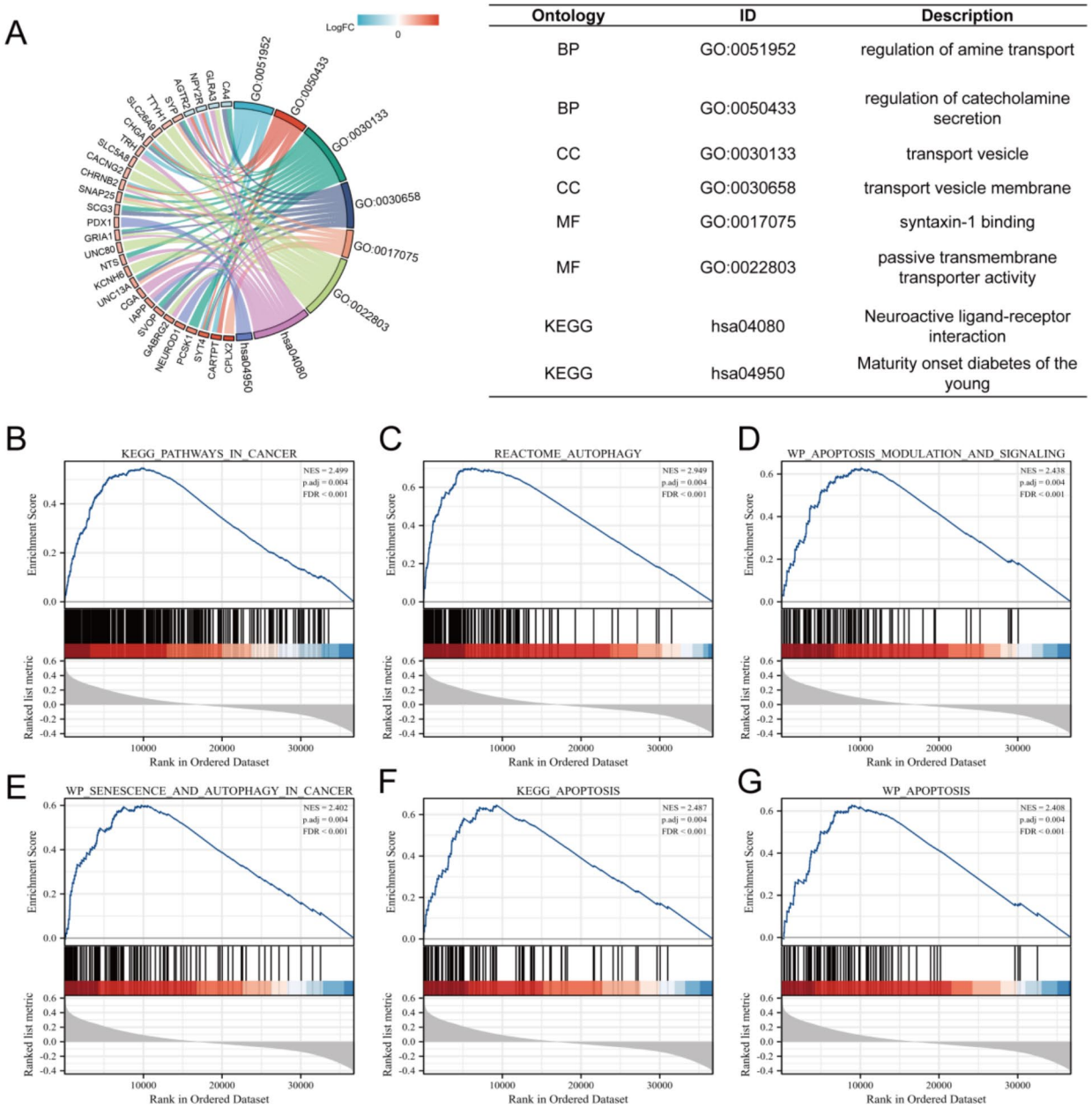

Ontology	ID	Description
BP	GO:0051952	regulation of amine transport
BP	GO:0050433	regulation of catecholamine secretion
CC	GO:0030133	transport vesicle
CC	GO:0030658	transport vesicle membrane
MF	GO:0017075	syntaxin-1 binding
MF	GO:0022803	passive transmembrane transporter activity
KEGG	hsa04080	Neuroactive ligand-receptor interaction
KEGG	hsa04950	Maturity onset diabetes of the young

Fig. 4 Enrichment plots from the KEGG/GO and GSEA in TCGA. (**A**) KEGG/GO enrichment analysis of APOO Related Genes in BRCA. (**B**–**G**) Various pathways and biological processes in BRCA with APOO Related Genes. (NES, normalized enrichment score; p.adj, adjusted *P* value; FDR, false discovery rate)

with transport vesicles and transport vesicle membranes, indicating a significant involvement in cellular trafficking.

The molecular functions of these genes include syntaxin-1 binding and passive transmembrane transporter activity, underscoring their role in cellular communication and substance transport across membranes. Furthermore, the enrichment analysis linked APOO interactive genes to significant pathways like Neuroactive ligand-receptor interaction and Maturity onset diabetes of the young. These findings provide valuable insights into the multifaceted roles of APOO and its associated genes, suggesting potential implications in various physiological and pathological processes.

GSEA identifies APOO-Related signaling pathways

In order to explore APOO-related pathways in BRCA, we performed GSEA on the DEGs between APOO-high and APOO-low expression groups and detected significant pathways at adjusted $P<0.05$ and FDR value <0.25, the gene set collection C2 from the Molecular Signatures Database v6.1 (MSigDB) was used. Pathways differentially enriched in the APOO high expression phenotype include *KEGG pathways in cancer*, *Reactome autophagy*, *WP apoptosis modulation and signaling*, *WP senescence and autophagy in cancer*, *KEGG apoptosis and WP apoptosis* (Fig. 4B–G). These findings suggested that APOO may be closely related to the apoptosis and autophagy signaling pathways.

Knockdown of APOO promotes apoptosis in BRCA cell lines

Previous bioinformatics analysis results have revealed that the APOO high expression phenotype is associated with effects on autophagy and apoptosis. In our experiment, siRNA-APOO decreased bcl2 expression and elevated bax and cleaved-caspase3 expression significantly (Fig. 5A). Additionally, the results of TUNEL assays were consistent with western blot results (Fig. 5B). We hypothesized that the cells with knockdown of APOO would show diminished resistance to apoptosis.

Knockdown of APOO suppresses autophagy in BRCA cell lines

Crosstalk exists between autophagy and apoptosis. Compared with the NC control group cells, BRCA cells transfected with siRNA-APOO showed distinct inhibition of ATG7, Beclin1 and LC3 II/I expression, and p62 expression was increased (Fig. 6A). Using immunofluorescence microscopy, we examined the variations in autophagy in BRCA cells transfected with mRFP-GFP-LC3. When the autophagosome membrane is formed, it expresses LC3 with green and red fluorescence, whereas GFP is quenched in functional autophagosomal lysosomes due

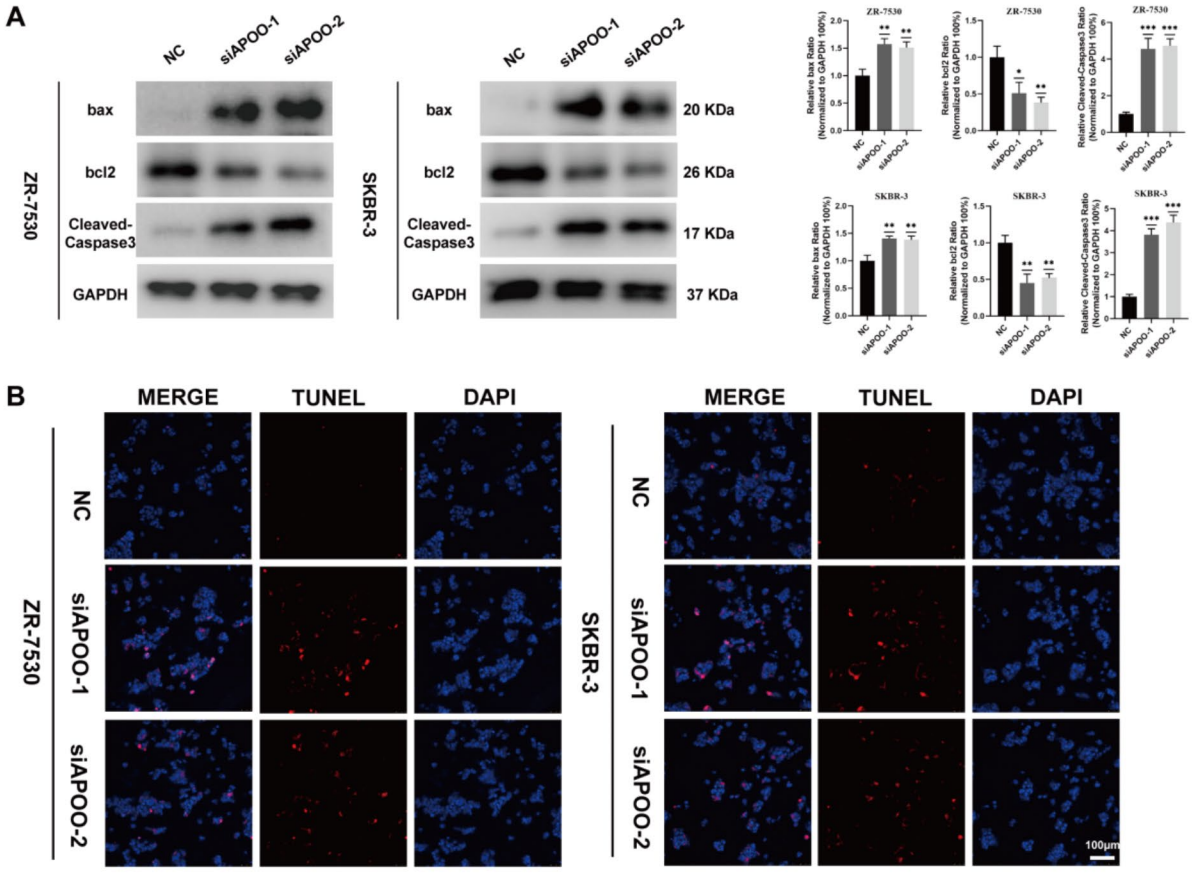

Fig. 5 APOO promotes apoptosis of BRCA cell lines. (**A**) The apoptosis-related proteins in siRNA-NC or siRNA-APOO cells as determined by western blotting. (**B**) TUNEL assay showing the number of apoptotic cells in different groups. (*$p<0.05$, **$p<0.01$, ***$p<0.001$)

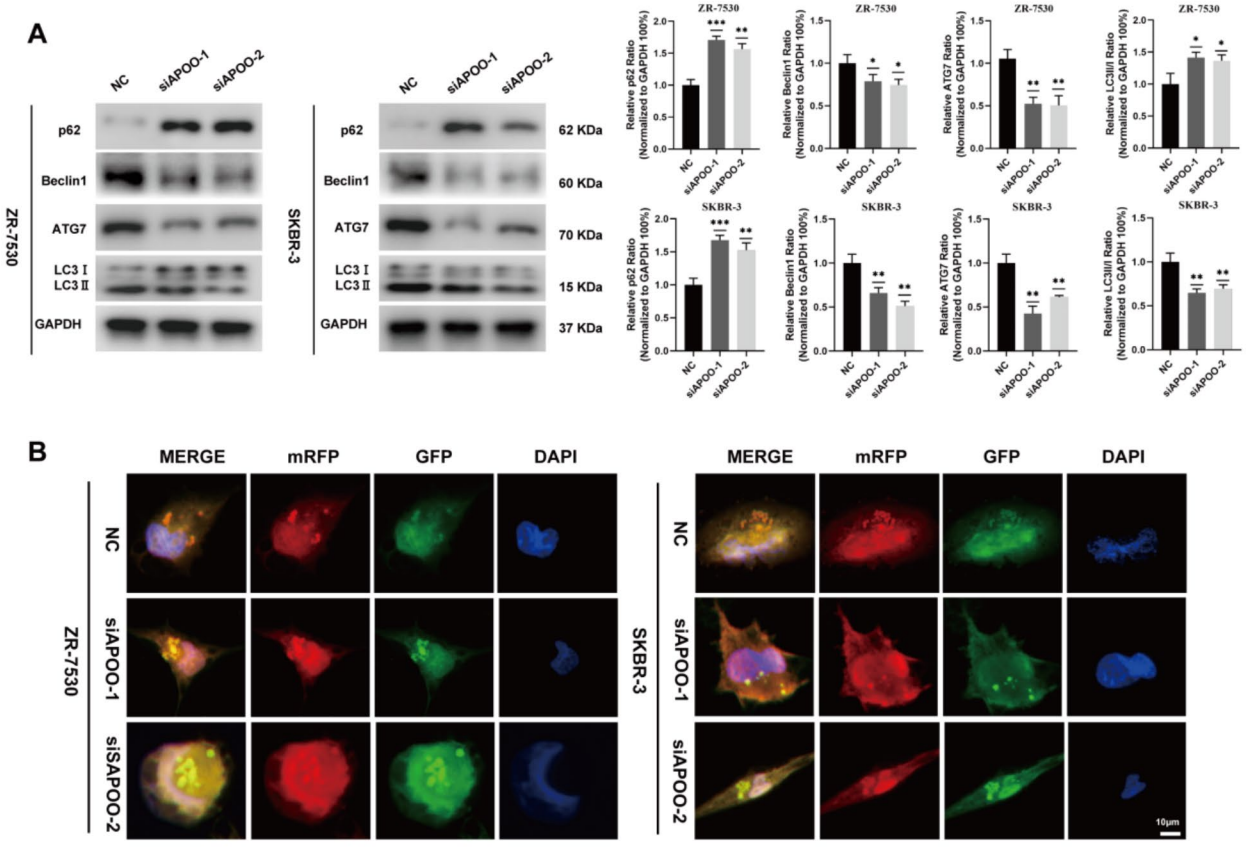

Fig. 6 APOO suppresses autophagy of BRCA cell lines. (**A**) The autophagy-related proteins in siNC or siRNA-APOO cells as determined by western blotting. (**B**) Alveolar macrophages were transfected with an adenovirus expressing mRFP-GFP-LC3. (*$p < 0.05$, **$p < 0.01$, ***$p < 0.001$)

to acidic pH. The formation of red puncta indicating autolysosomes was not obviously observed when BRCA cells were treated with siRNA-APOO (Fig. 6B). In summary, these results revealed that knockdown of APOO suppressed autophagy.

Discussion

Abnormal cancer cell metabolism, exemplified by the "Warburg effect" and its associated altered glucose metabolism, is a key feature of malignant tumors. Lipid metabolism has similarly gained prominence in tumor metabolism research. Lipid-binding proteins, crucial in transporting plasma lipids to various tissues for metabolism and utilization, can significantly influence disease progression when dysregulated. For example, APOE is known to activate Akt phosphorylation, and APOL6 can regulate autophagy, both playing vital roles in tumor initiation and progression [17, 18]. In our study, we investigated the role of APOO in BRCA. We found that APOO was highly expressed in BRCA tissues and was associated with cell growth, migration, invasion, and apoptosis in BRCA cells.

Alterations in lipid metabolism contribute to tumor growth, migration, invasion, metastasis, and immune evasion. In tumors, dysregulated lipid metabolism can lead to an accumulation of free fatty acids, inducing oxidative stress through increased reactive oxygen species (ROS) production [19]. This oxidative stress can damage DNA, proteins, and lipids [20], further disrupting lipid metabolism and increasing lipid content in tumor cells [21], thereby enhancing tumor growth and metastasis.

Autophagy, a vital cellular degradation process, maintains cellular homeostasis by degrading and recycling various components, including lipids, proteins, and organelles. It is essential in nutrient response and hypoxia, providing energy and nutrients for cell survival and growth [22]. The interplay between lipid metabolism and autophagy is evident, with molecules like

sphingosine inhibiting autophagosome maturation and phosphatidylinositol-4,5-bisphosphate (PI-4,5-P2) promoting autophagy to regulate lipid metabolism [23, 24]. Literature also suggests that autophagy-related molecule PPARα regulates genes involved in fatty acid β-oxidation, influencing lipid autophagy and fatty acid oxidation [25, 26]. Knockout of ATG7 or ATG1 can inhibit cellular autophagy, leading to the accumulation of NCoR1 and suppression of PPARα expression, resulting in impaired lipid oxidation [27]. In our research, we found that pathways differentially enriched in BRCA with high APOO expression were predominantly linked to autophagy. We thus explored APOO's role in autophagy by knocking down its expression in BRCA cells and analyzing autophagy-related molecules through protein quantification and immunofluorescence. Our results indicated a significant inhibition of autophagy upon APOO knockdown, suggesting APOO's close involvement in the autophagy signaling pathway.

This study highlights APOO's high expression in BRCA patients, linking elevated APOO levels with poor prognosis. By silencing APOO using siRNA, we observed decreased proliferation and migration in BRCA cells, alongside cell cycle alterations. Moreover, APOO knockdown led to reduced autophagy and increased apoptosis. Collectively, these findings suggest that APOO, acting as an oncogene, plays a crucial role in the occurrence and development of BRCA .

Limitations

Considerations should be given to some limitations of this study. Firstly, the quality and consistency of the data in the TCGA database used in this study is an important issue. Data from different batches may have technical biases, requiring rigorous data cleaning and standardization in the preprocessing stage. Meanwhile, although breast cancer cell lines are often used in breast cancer research, the establishment of cancer cell lines involves the selection of tumor cells adapted to in vitro culture conditions, thus cancer cell lines are generally considered to be homogeneous and unable to maintain the heterogeneity of the original tumor. Therefore, the gene expression changes related to APOO in our study may not fully reflect the changes occurring in human breast cancer tissue. Secondly, we did not use sequencing to determine the regulatory mechanism of APOO in breast cancer cells that were not subjected to APOO knockdown treatment; therefore, the exact mechanism involved in the APOO-dependent changes in breast cancer cells remains unclear. Finally, our study observed that high APOO expression was associated with poor prognosis in a specific subset of patients. The existence of this correlation may reflect the potential biological role of APOO in tumor development and progression. Further research may help elucidate the exact mechanisms of APOO in this subset of patients and provide more clues for personalized treatment targeting this patient population.

Conclusion

Our findings suggest that APOO enhances cell growth and migration while inhibiting apoptosis in BRCA cells. Additionally, APOO appears to influence BRCA progression through the autophagy pathway. Moving beyond bioinformatics predictions, we established the biological function of APOO using a cell model. To corroborate these findings, further research using an appropriate animal model and clinical studies is warranted. Overall, our data points to the possibility of a novel therapeutic approach for BRCA, opening new avenues for treatment strategies.

Abbreviations

APOO	Apolipoprotein O
ROC	Receiver operating characteristic
BRCA	Breast cancer
AUC	Area under curve
FDR	False discovery rate
PFI	Progression-free interval
OS	Overall survival
DSS	Disease-specific survival
C-index	Concordance index
HRs	Hazard ratios
DEG	Differential expression analysis
p.adj	Adjusted P value
NES	Normalized enrichment score

Supplementary Information

The online version contains supplementary material available at https://doi.org/10.1186/s12920-024-02047-7.

Supplementary Material 1

Supplementary Material 2

Author contributions

YB and QT was primarily responsible for the study design and bioinformatic analysis. LZ participated in molecular biology experiments. JH and WJ W wrote the draft of the manuscript, JY and LQ L proofreading and revising the manuscript. All authors contributed to the article and approved the submitted version.

Funding

This study was supported by the National Natural Science Foundation of China (Grant No. 82203292).

Data availability

The data sets generated and analyzed during the present study are available from the corresponding author on reasonable request.

Declarations

Ethics approval and consent to participate

All experimental protocols were approved by the Ethics Committee of the First Affiliated Hospital of Sun Yat-sen University, and conducted according to the Declaration of Helsinki.

Consent for publication
Not applicable.

Competing interests
The authors declare no competing interests.

dCompeting interests
The authors declare that they have no competing interest.

Author details
1 Laboratory of Department of Surgery, the First Affiliated Hospital of Sun Yat-sen University, Guangzhou, Guangdong 510080, China; 2 Department of Thyroid and Breast Surgery, the First Affiliated Hospital of Sun Yat-sen University, Guangzhou, Guangdong 510080, China; 3 Department of General Surgery, Xinqiao Hospital, Army Medical University, Chongqing 400037, China, 4 Department of Anesthesiology, Guiqian International General Hospital, Guiyang, 550000, Guizhou, China.

Received: 18 March 2024 / Accepted: 7 November 2024
Published online: 18 November 2024

References

1. Siegel RL, Miller KD, Fuchs HE, Jemal A. Cancer statistics, 2022. Ca Cancer J Clin. 2022;72(1):7–33. https://doi.org/10.3322/caac.21708.
2. Bray F, Ferlay J, Soerjomataram I, Siegel RL, Torre LA, Jemal A. Global cancer statistics 2018: GLOBOCAN estimates of incidence and mortality worldwide for 36 cancers in 185 countries. Ca Cancer J Clin. 2018;68(6):394–424. https://doi.org/10.3322/caac.21492.
3. Jeibouei S, Akbari ME, Kalbasi A, Aref AR, Ajoudanian M, Rezvani A et al. Personalized medicine in breast cancer: pharmacogenomics approaches. Pharmgenomics Pers Med. 2019;12:59-73.10.2147/PGPM.S167886.
4. Prat A, Pineda E, Adamo B, Galvan P, Fernandez A, Gaba L, et al. Clinical implications of the intrinsic molecular subtypes of breast cancer. Breast. 2015;24(Suppl 2):S26–35. https://doi.org/10.1016/j.breast.2015.07.008.
5. Zhang X, Niu Z, Qin H, Fan J, Wang M, Zhang B et al. Subtype-Based Prognostic Analysis of Cell-in-Cell Structures in Early Breast Cancer. Front Oncol. 2019;9:895.10.3389/fonc.2019.00895.
6. Wuerstlein R, Kates R, Gluz O, Grischke EM, Schem C, Thill M et al. Strong impact of MammaPrint and BluePrint on treatment decisions in luminal early breast cancer: results of the WSG-PRIMe study. Breast Cancer Res Treat. 2019;175(2):389-399.10.1007/s10549-018-05075-x.
7. Laplante M, Sabatini DM. An emerging role of mTOR in lipid biosynthesis. Curr Biol. 2009;19(22):R1046–52. https://doi.org/10.1016/j.cub.2009.09.058.
8. Menendez JA. Fine-tuning the lipogenic/lipolytic balance to optimize the metabolic requirements of cancer cell growth: molecular mechanisms and therapeutic perspectives. Biochim Biophys Acta. 2010;1801(3):381–91. https://doi.org/10.1016/j.bbalip.2009.09.005.
9. Philip-Couderc P, Smih F, Pelat M, Vidal C, Verwaerde P, Pathak A et al. Cardiac transcriptome analysis in obesity-related hypertension. Hypertension. 2003;41(3):414-421.10.1161/01.HYP.0000057573.32425.95.
10. Lamant M, Smih F, Harmancey R, Philip-Couderc P, Pathak A, Roncalli J, et al. ApoO, a novel apolipoprotein, is an original glycoprotein up-regulated by diabetes in human heart. J Biol Chem. 2006;281(47):36289–302. https://doi.org/10.1074/jbc.M510861200.
11. Turkieh A, Caubere C, Barutaut M, Desmoulin F, Harmancey R, Galinier M, et al. Apolipoprotein O is mitochondrial and promotes lipotoxicity in heart. J Clin Invest. 2014;124(5):2277–86. https://doi.org/10.1172/JCI74668.
12. Ott C, Dorsch E, Fraunholz M, Straub S, Kozjak-Pavlovic V. Detailed analysis of the human mitochondrial contact site complex indicate a hierarchy of subunits. PLoS ONE. 2015;10(3):e120213. https://doi.org/10.1371/journal.pone.0120213.
13. Koob S, Barrera M, Anand R, Reichert AS. The non-glycosylated isoform of MIC26 is a constituent of the mammalian MICOS complex and promotes formation of crista junctions. Biochim Biophys Acta. 2015;1853(7):1551-1563.10.1016/j.bbamcr.2015.03.004.
14. Liu Y, Xiong Z, Zhou W, Chen Y, Huang Q, Wu Y. Role of apolipoprotein O in autophagy via the p38 mitogen-activated protein kinase signaling pathway in myocardial infarction. Clin (Sao Paulo). 2022;77:100046. https://doi.org/10.1016/j.clinsp.2022.100046.
15. Subramanian A, Tamayo P, Mootha VK, Mukherjee S, Ebert BL, Gillette MA et al. Gene set enrichment analysis: a knowledge-based approach for interpreting genome-wide expression profiles. Proc Natl Acad Sci U S A. 2005;102(43):15545-15550.10.1073/pnas.0506580102.
16. Yu G, Wang LG, Han Y, He QY. clusterProfiler: an R package for comparing biological themes among gene clusters. Omics. 2012;16(5):284-287.10.1089/omi.2011.0118.
17. Laffont I, Takahashi M, Shibukawa Y, Honke K, Shuvaev VV, Siest G et al. Apolipoprotein E activates Akt pathway in neuro-2a in an isoform-specific manner. Biochem Biophys Res Commun. 2002;292(1):83-87.10.1006/bbrc.2002.6586.
18. Zhaorigetu S, Yang Z, Toma I, McCaffrey TA, Hu CA. Apolipoprotein L6, induced in atherosclerotic lesions, promotes apoptosis and blocks Beclin 1-dependent autophagy in atherosclerotic cells. J Biol Chem. 2011;286(31):27389-27398.10.1074/jbc.M110.210245.
19. Gao Y, Song Z, Jia L, Tang Y, Wang C, Zhao X et al. Self-amplified ROS production from fatty acid oxidation enhanced tumor immunotherapy by atorvastatin/PD-L1 siRNA lipopeptide nanoplexes. Biomaterials. 2022;291:121902.10.1016/j.biomaterials.2022.121902.
20. Nakamura H, Takada K. Reactive oxygen species in cancer: current findings and future directions. Cancer Sci. 2021;112(10):3945–52. https://doi.org/10.1111/cas.15068.
21. Xia L, Oyang L, Lin J, Tan S, Han Y, Wu N et al. The cancer metabolic reprogramming and immune response. Mol Cancer. 2021;20(1):28.10.1186/s12943-021-01316-8.
22. Mizushima N, Komatsu M. Autophagy: renovation of cells and tissues. Cell. 2011;147(4):728–41. https://doi.org/10.1016/j.cell.2011.10.026.
23. Merrill AJ. Sphingolipid and glycosphingolipid metabolic pathways in the era of sphingolipidomics. Chem Rev. 2011;111(10):6387–422. https://doi.org/10.1021/cr2002917.
24. Lundquist MR, Goncalves MD, Loughran RM, Possik E, Vijayaraghavan T, Yang A et al. Phosphatidylinositol-5-Phosphate 4-Kinases Regulate Cellular Lipid Metabolism By Facilitating Autophagy. Mol Cell. 2018;70(3):531-544.10.1016/j.molcel.2018.03.037.
25. Settembre C, De Cegli R, Mansueto G, Saha PK, Vetrini F, Visvikis O et al. TFEB controls cellular lipid metabolism through a starvation-induced autoregulatory loop. Nat Cell Biol. 2013;15(6):647-658.10.1038/ncb2718.
26. Barthel A, Schmoll D, Unterman TG. FoxO proteins in insulin action and metabolism. Trends Endocrinol Metab. 2005;16(4):183–9. https://doi.org/10.1016/j.tem.2005.03.010.
27. Saito T, Kuma A, Sugiura Y, Ichimura Y, Obata M, Kitamura H et al. Autophagy regulates lipid metabolism through selective turnover of NCoR1. Nat Commun. 2019;10(1):1567.10.1038/s41467-019-08829-3.

Publisher's note